CrossMark

ORIGINAL PAPER

A comparative study of models to predict storm impact on beaches

Iñaki de Santiago[1] · Denis Morichon[1] · Stéphane Abadie[1] ·
Ad J. H. M. Reniers[2] · Pedro Liria[3]

Abstract The storm impact scale of Sallenger (J Coast Res 890–895, 2000) was tested on a partially engineered beach. This scale is supposed to provide a convenient tool for coastal managers to categorize the storm impact at the shore. It is based on the relation between the elevation of storm wave runup and the elevation of a critical geomorphic or man-made structures in the present study. Two different approaches were tested to estimate the elevation of extreme storm wave runup: (1) a parametric model based on offshore wave conditions and local beach slope and (2) the XBeach process-based model that solves implicitly the runup. The study shows comparisons between impact regimes computed with the two methods and those derived from video observations acquired during 2 weeks while the site was battered by three consecutive storms. Storms scenario including wave conditions with higher return periods and different tidal range were also investigated. The advantages and disadvantages of the two methods used to compute extreme water level are then compared, and guidelines for the development of early warning system are drawn.

Keywords Storm impact · XBeach · Extreme runup · Risk management · Urbanized beach

1 Introduction

While several studies have shown that sea level rise is a well-accepted indicator and a relevant variable of the climate change, the meteorological changes and the increase in intensity and frequency of storms are still debatable (Bengtsson et al. 2009). However,

✉ Iñaki de Santiago
  inaki.desantiagogonzalez@univ-pau.fr

[1] Laboratoire des Sciences de l'Ingénieur Appliquées à la Mécanique et au génie Electrique-IPRA, EA4581, Université de Pau et des Pays de l'Adour, 64600 Anglet, France

[2] Civil Engineering and Geosciences, Delft University of Technology, Delft, The Netherlands

[3] AZTI-Tecnalia Herrera Kaia, Portualdea z/g, 20110 Pasaia, Gipuzkoa, Spain

⚙ Springer

even if the current characteristics of storms will not vary, it is reasonable to consider that an increase in sea level will cause an intensification of the impact of storms on coastal zones by for example amplifying the effect of storm surges. This is especially true, as the level of resilience of coastal zones can be modified by the combination of human uses and development. Consequently, coasts are expected to be exposed to increasing risks such as coastal flooding, structure damages and beach erosion. The possibility to forecast beach response to wave actions during highly energetic conditions is thus of great societal relevance and vital for developing an appropriate strategy of coastal management and planning (Ferreira 2005).

The assessment of the potential severity of storms, in particular to set up alert or temporary protection measures in good time seems to be a challenging task as the beach response is dependent on multiple physical, structural and morphological parameters interacting at different spatial and time scales. For instance, the level of storm impact will depend in particular on the beach shape and outer bar morphologies (Smit 2010; Morton 2002; Castelle et al. 2015), the forced coastal hydrodynamics (Loureiro et al. 2012), the balance between storm frequency and recovery rates (Ferreira 2005; Vousdoukas et al. 2012a; Coco et al. 2014; Splinter et al. 2014; Karunarathna et al. 2014). However, from coastal managers point of view, it is not necessarily required to consider all the above mentioned parameters to develop an operational early warning system (EWS). Indeed, the vulnerability of a beach to storm impact can be related to storm threshold values above which important morphological changes or damages to man-made structures can occur (Ciavola et al. 2011b). This implies to translate physical values, related to hydraulic conditions and beach characteristics, into hazards levels or vulnerability.

A storm impact prediction system was developed and tested on nine pilot sites in the framework of the FP7 MICORE project (www.micore.eu). The system is based on a series of Storm Impact Indicators developed following the methodology of van Koningsveld et al. (2005) that used the storm impact scale of Sallenger (2000). According to this scale, the range of potential beach responses is function of the relation between the elevation of characteristics points along a beach profile and the maximum water level, hereinafter referred to extreme runup, reached during a storm. The first lines of defence on natural beaches usually correspond to the sand dune. Indeed, for this type of beach configuration, the dune allows to minimize the threat of human lives and damage of properties. For artificial beach, usually the coastal amenities are protected by a concrete structure like a seawall. The natural or engineered protection will provide safe conditions for resident and properties behind this limit if the maximum water elevation is lower than their highest points. The maximum water elevation or extreme runup that is expected to be reached during a storm is then computed either with a numerical model (Cohn and Ruggiero 2016; Guimarães et al. 2015 among others) or with an empirical formulation (Holman 1986; Nielsen and Hanslow 1991; Stockdon et al. 2006 among others). Currently, the XBeach model (Roelvink et al. 2009) is probably one of the most widely used process-based model. It was used on a wide variety of beach types in various coastal environments (Williams et al. 2012; Beevers et al. 2016; Cohn and Ruggiero 2016 among others). This model is a site-specific model which implies a heavy calibration procedure. The empirical formula is usually easier to apply as they simply depend on offshore wave characteristics and quantities representative of the morphologic features. However, they cannot account for the influence of the rapid morphology evolution on the hydrodynamics which are characteristics of storm events. The Stockdon et al. (2006) formulation (hereinafter referred to S2006) has proved its efficiency to estimate wave runup on different sites (Stockdon et al.

2006, 2014; Senechal et al. 2011) combining the contribution of incident short waves and infragravity waves in a single formula relatively easy to implement.

Recently, Poelhekke et al. (2016) have proposed an alternative approach to predict coastal hazards based on a probabilistic method using a Bayesian network. This approach gives promising results for the development of EWS, while highlighting the need for the collection of an extensive set of observed or hindcasted data together with onshore hazards observations or predictions. Unfortunately, simultaneous historical data of hydraulic conditions and onshore hazards are usually sparse.

In this paper, we adopted an approach similar to the storm impact prediction system developed in MICORE. The main focus of the study is to compare storm impact regimes (hereinafter referred to as SIR) computed using both XBeach model and the S2006 formulation in order to provide some guidelines for the development of EWS. The study is based on a set of video and topographic data that were acquired during a sequence of storms that battered the partially engineered beach of Zarautz (Northern Spain) during the winter 2012–2013. This embayed beach presents a special feature, since it is partly backed by a sand dune, while a seawall is present along the rest of the beach. The study site is briefly described in Sect. 2. The model developed to obtain nearshore wave data, the approach used to define the storm characteristics and the method used to derive water level elevation from video images are explained in Sect. 3. The Sallenger scale, the S2006 empirical formula and the XBeach model used to compute the extreme water elevation are presented in Sect. 4. We also describe the methodology used to assess SIR from video images. The results are given in Sect. 5 and discussed in Sect. 6. Finally, the main results of the study are summarized in Sect. 7.

2 Study site

The study area is located on the northern Spanish coast. This region presents a coastline with complex geological features including pocket beaches of different dimensions and shapes. Coastal structures (i.e. seawall, groyne, breakwater) are present at different scales and only a few beaches are still pristine. The beach selected for the study is a North–Northwest-oriented pocket beach located in the town of Zarautz in the Bay of Biscay (Northern Spain) (Fig. 1). This coastal embayment stretches over 2 Km between two rocky headlands. Sand dunes, located on the eastern part, cover 30% of the beach. The remaining 70% is backed by a concrete vertical seawall of varying height. At the western part, the top of the wall is almost 4 m above the mean sea level, while at the eastern part it reaches up to 9 m.

The distribution of sediment size varies along the beach. The mean sediment grain size (d_{50}) ranges between 0.2 and 0.45 mm. The finest fraction is located at the western side of the beach, in the most protected area. The slope (β) of the beach ranges from 0.02 in the western engineered part to 0.06 in the eastern natural part. The beach morphology is mostly double-barred with both bars able to go through all the states within the intermediate classification of the Wright and Short (1984). Various preferred locations of rip channel formation were identified along the beach suggesting that the effects of the headlands can propagate towards the centre of the bay. Finally, the western engineered and more sheltered section of the beach sometimes exhibits a different beach state compared to that of the eastern section (de Santiago et al. 2013).
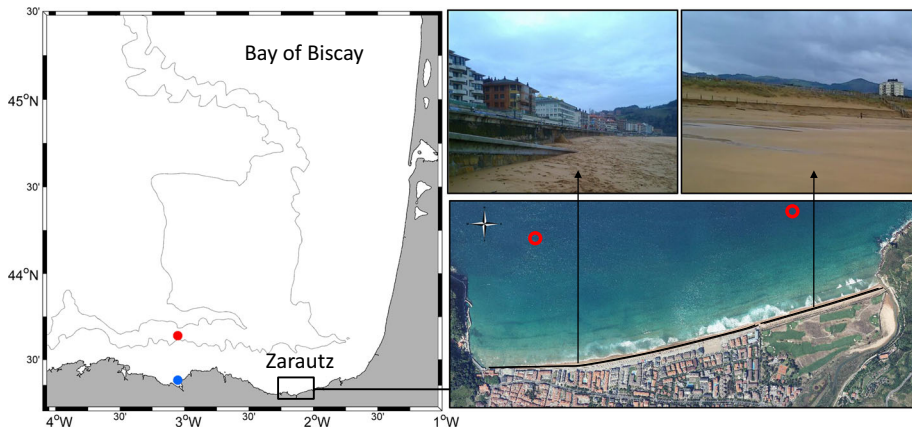
Fig. 1 Location and description of the study area. *Left panel* shows the Bay of Biscay with the location of the study site (*black box*), the Bilbao-Vizcaya wave buoy (*red dot*) and the tidal gauge (*blue dot*). The *low-right panel* shows the beach of Zarautz and the location of the directional wave gauges (*red circles*). The *two up-right panels* illustrate the two different sections of the beach, engineered (*left*) and natural (*right*)

Tides are semidiurnal and mesotidal. Sea levels are referred to the Spanish Topographic Institute, 0 reference level. Hence, the mean sea level at the study site corresponds to 0.33 m, with a maximum tidal elevation of 2.8 m and a maximum spring tidal range of 4.7 m. The nearest buoy of the study site is the Bilbao-Vizcaya buoy moored in 600 m water depth (Fig. 1). The wave data provided by Spanish port authorities encompasses 23 years (1991–2013) of statistical parameters (H_s, T_p, θ_p etc.) and 10 years (2004–2013) of wave spectra. The most frequent sea states have significant wave heights between 1 and 2 m and peak periods varying between 8.5 and 11 s. The 95% of the waves are confined between W–N directions, where two main directions are dominant, NW–WNW.

The intensity and frequency of storms are seasonally variable. This is explained by the influence of the Azores High and the Iceland Low that predominantly govern the North Atlantic wave climate (Wooster et al. 1976; Vitorino et al. 2002; Woolf et al. 2002). The wave climate at this region is highly energetic, especially during autumn and winter seasons. The most energetic events ($H_s > 3.3$ m) are linked to larger periods ($T_p = 12.5$–14 s) coming from the same direction as mean conditions but limited to a narrower directional band.

3 Material and methods

3.1 Wave data

The nearshore wave data characteristics (H_s, T_p, θ_p) used to compute extreme water levels with the calibrated XBeach model and the S2006 formula were derived from the deep water Bilbao-Vizcaya buoy (Fig. 1). These offshore wave spectra were propagated to the nearshore by means of a transformation matrix obtained from the monochromatic version of REF/DIF, a parabolic refraction–diffraction model (Kirby et al. 1994). Since the model is linear, a transformation matrix can be derived propagating different frequencies and directions with an incident wave of unit amplitude (O'Reilly and Guza 1993). The resulting
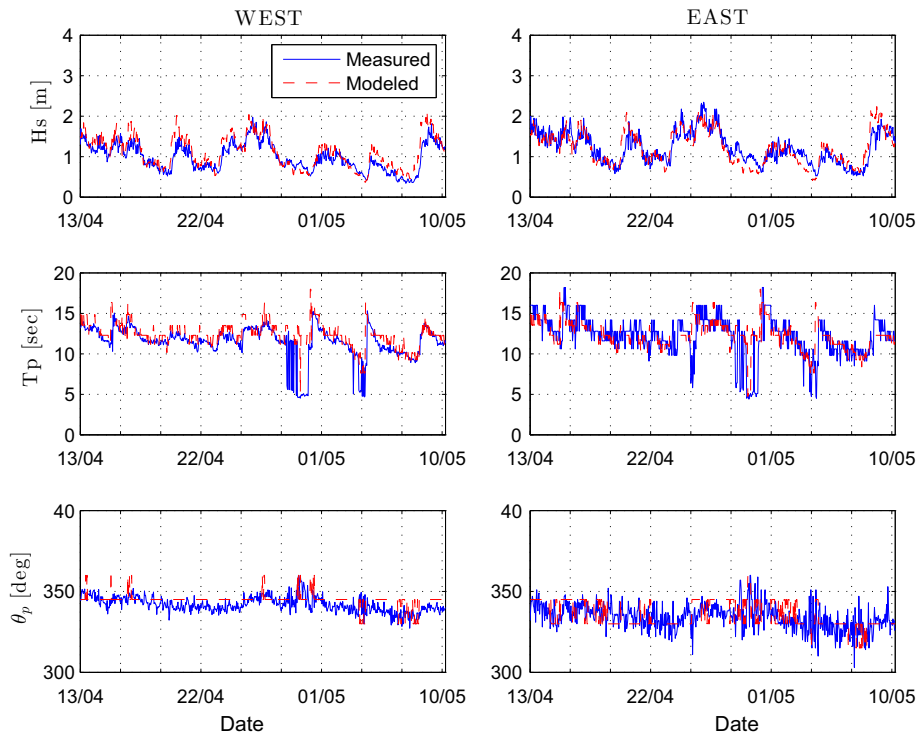
Fig. 2 Validation of the 'transformation matrix' methodology performance against the real measures at the beach of Zarautz during a 1-month period

transformation matrix can then be used to simulate the propagation of a given offshore directional spectrum by applying these coefficients, allowing to significantly limit the computational time.

   The validation of the wave model was performed by comparing calculated nearshore wave characteristics with measurements obtained with two acoustic wave recorders (Nortek Awac 1000 and Teledyne RDI 600). The two wave recorders were moored at about 18 m at each side of the beach during 1 month. Figure 2 displays the comparison between the computed and measured wave characteristics at the two positions. The results highlight the robustness of the method with a root mean square error (RMSE) lower than 0.25 m, 2.25 s and 9° for H_s, T_p and θ_p, respectively. These results are consistent with other studies performed on different sites (Vousdoukas et al. 2012b). The measured alongshore variability of wave height is well reproduced by the wave model with lower wave heights on the western side of the bay, which is more sheltered.

3.2 Storm waves conditions

The nearshore wave characteristics were first analysed (Sect. 5) to characterize the storms that battered the beach during the study period. The definition of storm wave conditions for a given site requires to separate the ordinary wave conditions from extreme event conditions. Generally, a given event is considered extreme if the wave height is higher than a threshold value. Then, if these conditions are maintained during a significant time it would

be accepted as a storm. In literature, the threshold value corresponds to the value of H_s that is exceeded 8–10% of time (Rangel-Buitrago and Anfuso 2011a; Dorsch et al. 2008), or to the minimum H_s which results in a measurable beach face erosion (Dolan and Davis 1992; Rangel-Buitrago and Anfuso 2011b). In this study, a threshold value of 2.1 m, corresponding to the nearshore H_s value exceeded 10% of time was applied to discriminate between arbitrary waves and storm waves. Since the tidal regime is semidiurnal, it was assumed that the minimum extreme wave duration to be considered as a storm should be at least of 12 h (Rangel-Buitrago and Anfuso 2011a) to take into account the action of the event over at least a whole tidal cycle. Finally, a minimum inter-storm period of 24 h was established to ensure an independence between events. Hence, in a case where two consecutive storms are separated by less than 24 h, it is considered a single storm. This inter-storm interval is comparable to mid-latitude extreme events (e.g. mid-latitude cyclones) occurring on a time scale of 24 h approximately (Oke 1987). In order to calculate the storm magnitude (i.e. the total wave energy reaching the coast during the storm duration), each storm was properly isolated taking into account the above mentioned rules. Then, the storm magnitude was calculated as follows:

$$\int_0^{t_d} E c_g \, \mathrm{d}t \tag{1}$$

where the formula represents the integration of the energy flux formed by the wave energy (E) and the wave group celerity (c_g) over the total storm duration (t_d). The results of the storm analysis are given in Sect. 5.1.

3.3 Water elevation derived from video images

The in situ data used in Sect. 4.3 to test the ability of the calibrated XBeach model to compute runup elevation were derived from the combination of video images and surveyed beach profiles. Video techniques have been widely used to collect runup data on a variety of sites (Holman and Guza 1984; Holland et al. 1995; Stockdon et al. 2006; Vousdoukas 2014). Usually, the runup elevation is obtained from a timestack image, which represents the temporal pixel intensity collected at 1 Hz frequency along a cross-shore transect spanning the swash zone. The leading edge of runup is detected and converted to time series of water elevation using photogrammetric relationships. It is then possible to calculate runup statistics.

A shore-based video system is operating on top of the western headland of the Zarautz beach at 90 m above the mean sea level since 2010 (de Santiago et al. 2013). The system is equipped with four cameras that point different sections of the beach, covering the shoaling, surf and swash zones. The image resolution ranges from 0.05 to 0.6 m for the angular (cross-shore) component and from 2 to 9 m for the radial (alongshore) component. Unfortunately, time stack images were not collected by the video system during the study period. However, time exposure (timex) images were collected each 20 min. The timex images were obtained by averaging frames collected at 0.5 Hz over a 20-min period. This type of images are commonly used to detect the shoreline position using a detection algorithm to delineate the shoreline based on colour intensity contrast between wet and dry pixels (Aarninkhof et al. 2003). The water elevation at the video-detected shoreline position can then be obtained from a topographic beach survey carried out at the time of video acquisition.

Fig. 3 Location of the eleven surveyed beach profiles used to calculate runup

For this purpose, detailed topographic surveys of eleven cross-shore beach profiles spaced 200 m apart (Fig. 3) were undertaken at low tide to cover the widest part of the profiles. The profiles were selected to be representative of the different sections (engineered/natural) of the beach. They extend from the base of the seawall or top of the dune up to, at least, the mean low water level. The surveys were carried out when the climatic conditions were favourable. Beach elevations were measured each 3 m with a Trimble RTK-GNSS (Real Time Kinematic Global Navigation Satellite System) with horizontal and vertical errors of less than 5 cm. The above mentioned approach was applied to estimate the water elevation variation for half a tidal cycle. This duration is assumed to be short enough for neglecting significant beach face changes as wave conditions were moderate ($H_s \approx 1.5$ m, $T_p \approx 12$ s).

4 Storm impact regimes (SIR) assessment

4.1 Storm impact scale

In this study, the storm impact scale of Sallenger (2000) is used to define the potential impact of a series of storms. We chose this model because it allows to relate external forcings to foreshore beach resilience on a relatively simple manner. For this reason, this scale appears to be well suited to serve as a base of a warning system. The scale has already been successfully used to assess the thresholds for storm impacts on sandy beaches with and without coastal structures (Ciavola et al. 2011a; Almeida et al. 2012). The scale distinguishes between different SIR which comprise in an ascending order of impact intensity, the (1) swash regime which corresponds to the extent of beach flooding during storms, (2) collision regime that can cause dune erosion or structure interaction, (3) overwash regime that can cause onshore sediment transport and wave overtopping and (4) inundation regime where beach and dune or seawall are constantly under water.

From a practical point of view, the distinction between the SIR is based on the relationship between representative high (R_{high}) and low (R_{low}) elevations of the landward margin of swash, and elevations of the highest (D_{high}) and lowest (D_{low}) part of the first line of defence of the case study (Fig. 4). In this study, D_{high} is defined by the elevation of the seawall (top of the dune) on the engineered zone (natural part), while D_{low} is represented
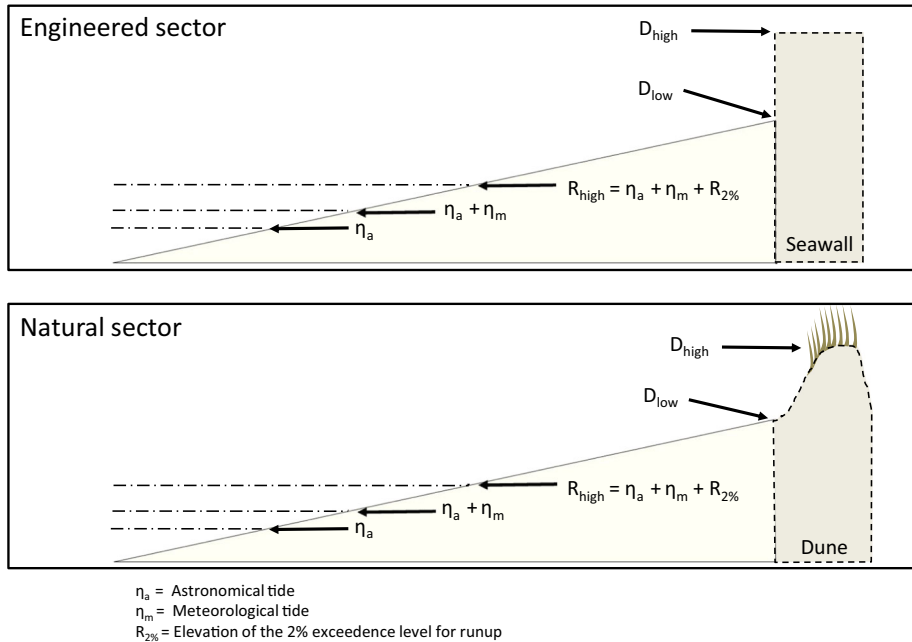
η_a = Astronomical tide
η_m = Meteorological tide
$R_{2\%}$ = Elevation of the 2% exceedence level for runup

Fig. 4 Definition sketch showing Sallenger ([2000]) basic parameters (R_{high}, D_{high} and D_{low}). The *dashed lines* represent the astronomical tide, meteorological tide and the total water level. The *top panel* is an illustration of the engineered zone. The *low panel* is an illustration of the natural zone. Modified from Sallenger ([2000])

by the base of the seawall (toe of the dune). The elevation of extreme water level (R_{high}) is given by the relation:

$$R_{high} = \eta + R_{2\%} \tag{2}$$

where η is the astronomical tide- and meteorological tide-induced water level and $R_{2\%}$ the 2% exceedance value of wave runup. In this study, η was given by a tidal gauge located ~ 100 km from the study site allowing to account for the large-scale storm surge.

The estimation of $R_{2\%}$ requires to account for the combined contribution of the maximum wave set-up (Longuet-Higgins and Stewart [1963]) and the swash elevation, which is defined as the vertical fluctuation of water level about the temporal mean. In the following, we present two different approaches to compute $R_{2\%}$ knowing the nearshore wave characteristics.

4.2 $R_{2\%}$ computation with the S2006 formula

The empirical formula S2006 (Stockdon et al. [2006]) was derived from statistics of water level, waves and beach slopes obtained during a series of field experiments intending to cover a wide range of environmental conditions. Its general form is given by:

$$R_{2\%} = 1.1 \left(\langle \eta \rangle + \frac{S}{2} \right) \tag{3}$$

where $\langle\eta\rangle$ denotes the maximum wave set-up component and S the swash component. The parametrization of S allows to account for both the contribution of incident waves and infragravity waves. Adding the parametrizations for each component the expression of $R_{2\%}$ is given by:

$$R_{2\%} = 1.1 \left(0.35\beta_{\mathrm{f}}(H_0 L_0)^{1/2} + \frac{\left[H_0 L_0 \left(0.563\beta_{\mathrm{f}}^2 + 0.004\right)\right]^{1/2}}{2} \right) \tag{4}$$

where β_{f} denotes the foreshore slope, here considered as the slope that exist between the high tidal level ($\eta_{90\%}$) and the low tidal level ($\eta_{10\%}$). The offshore wave height H_0 and wave length L_0 refer to offshore wave conditions corresponding to open beaches with shore parallel bathymetric isolines (Stockdon et al. 2006; Ruessink et al. 1998). In order to respect this hypothesis, a reverse shoaling approach was applied similar to Stockdon et al. (2006). This allows to estimate offshore significant wave height by propagating the computed nearshore significant wave height to deep water using linear wave theory assuming a shore-normal approach.

4.3 R_{high} computation with XBeach

The XBeach morphodynamic model (Roelvink et al. 2009) was designed to simulate beach changes during storms. The model implicitly resolves the different impact regimes that can occur (Sect. 4.1). More specifically, this time-dependent and process-based 2DH model solves coupled hydrodynamics and morphodynamics equations on the time scale of wave groups, including the contribution of infragravity waves which was shown to be significant in runup processes during storms (Raubenheimer and Guza 1996; Van Thiel de Vries et al. 2008). XBeach was recently used by Stockdon et al. (2014) to simulate storm-driven runup. In our study, the model was first calibrated using topographic data and the R_{high} values were then obtained by post processing the computed water elevations.

4.3.1 XBeach calibration

The model was run in a 2D mode to account for the alongshore non-uniformities of the Zarautz beach. The model input includes hourly nearshore wave spectra, obtained with the wave propagation model described in Sect. 3.1, and 5-min measured total water level given by the tidal gauge of Bilbao. The computational grid is irregular. In the cross-shore direction, the grid size varies from $\Delta x \approx 20$ m at the offshore boundary to $\Delta x \approx 1$ m at the shore. In the alongshore direction, the grid size is fixed to $\Delta y = 10$ m. The lateral boundaries are simulated as frictionless, impermeable walls. An absorbing-generating boundary condition is applied at the seaward model boundary (Van Dongeren and Svendsen 1997).

Model calibration was based on two topographic surveys carried out before and after a series of storms along the same eleven transects (Fig. 3) used to calculate the water elevation in Sect. 3.3. Due to the lack of a pre-storm bathymetry, it was estimated using the Beach Wizard model. This data assimilation model has previously shown to be an efficient tool to estimate the nearshore subtidal bathymetry on the basis of video-derived observations of wave roller energy dissipation and/or wave celerity (Van Dongeren et al. 2008; Sasso 2012; Morris 2013; Austin et al. 2012). In the present case, the Beach Wizard is only forced by wave roller dissipation maps. An alongshore non-uniform boundary option was

implemented (for more information the reader is referred to de Santiago 2014, section 5.4.2 Model adaptation) in the XBeach code (XBeach V19), in order to take into account the alongshore variation of wave conditions. The validation of the Beach Wizard model was performed using a bathymetry measured in June 2012 as an input. This bathymetry had a complex configuration with several rip currents along it. The target bathymetry used for the validation was measured on March 2013, also presenting several rip currents along the beach but at different locations and configuration. RMSE between surveyed and estimated depth ranges from 0.25 to 1 m at the surf zone. This concurs with previous studies (Aarninkhof et al. 2005; Van Dongeren et al. 2008) where the RMSE was around 0.5 m.

The XBeach model calibration consists in adjusting a number of free parameters. A total of $\sim$30 cases 2D and $\sim$35 cases 1D were tested with different values of γ_{ua} (influence of short wave skewness and asymmetry on sediment transport), γ (wave breaking parameter), eps (threshold depth for drying and flooding), h_{min} (Threshold water depth above which Stokes drift is included), wetslp (critical avalanching slope under water), dryslp (critical avalanching slope above water), nuhfac (viscosity switch for roller induced turbulent horizontal viscosity) and form (sediment transport equation applied by the model).

Good model agreement was obtained using $\gamma = 0.45$, eps $= 0.1$, $h_{min} = 0.1$ m, wetslp $= 0.2$, $\gamma_{ua} = 0.1$ and the rest of values set as default values. Model results are displayed in Fig. 5 for 4 profiles representative of the different sections of the beach. Overall,
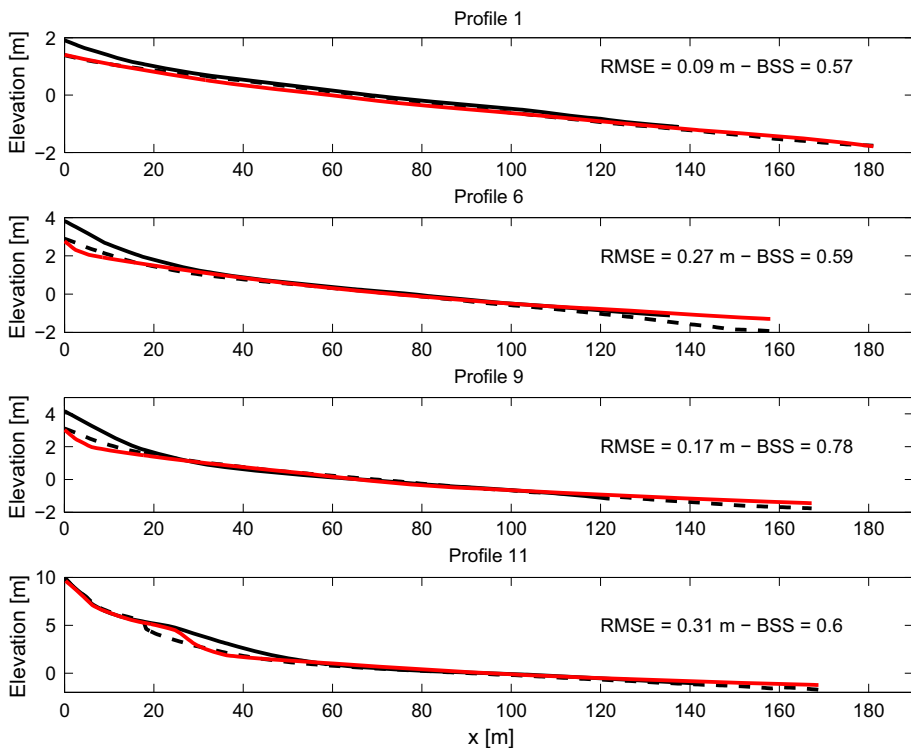

Fig. 5 Beach profiles measured before (*black solid line*) and after (*black dashed line*) a series of storms (Table 1) and the profiles computed with XBeach (*red solid line*) at four locations along the beach

the model predicts accurately the beach erosion in front the seawall for profiles 1,6 and 9. The dune toe retreat at profile 11 is also reproduced by the model, although the landward limit of the erosion is slightly underestimated. The averaged RMSE ($\overline{\text{RMSE}}$) between measured and modelled final was equal to 0.25 m. The alongshore model prediction skill is reasonably uniform with a $\overline{RMSE}$ of 0.22 m at the engineered sector and 0.28 m at the natural sector. These good results are confirmed by a relatively high Brier skill score (BSS) ranging between 0.5 and 0.8. The model showed to be more sensitive to the sediment transport formulation, wave breaking parameter and γ_{ua} which is consistent with previous studies (e.g. Vousdoukas et al. 2012b).

4.3.2 Water level elevation

The instantaneous water elevation level was calculated from the results of the calibrated XBeach model by detecting the shoreward-most wet point of the grid at a threshold of 10 cm each 2 s. This threshold depth was chosen according to sensitivity analysis carried out in Stockdon et al. (2014). The mean water level elevation R_{mean} was computed over a period of 20 min, that corresponds to the period over which the timex images are averaged (Sect. 3.3). The estimation of R_{mean} obtained from images fits well with the computed values (Fig. 6a). The overall RMSE error is of 0.56 m, although better results are obtained
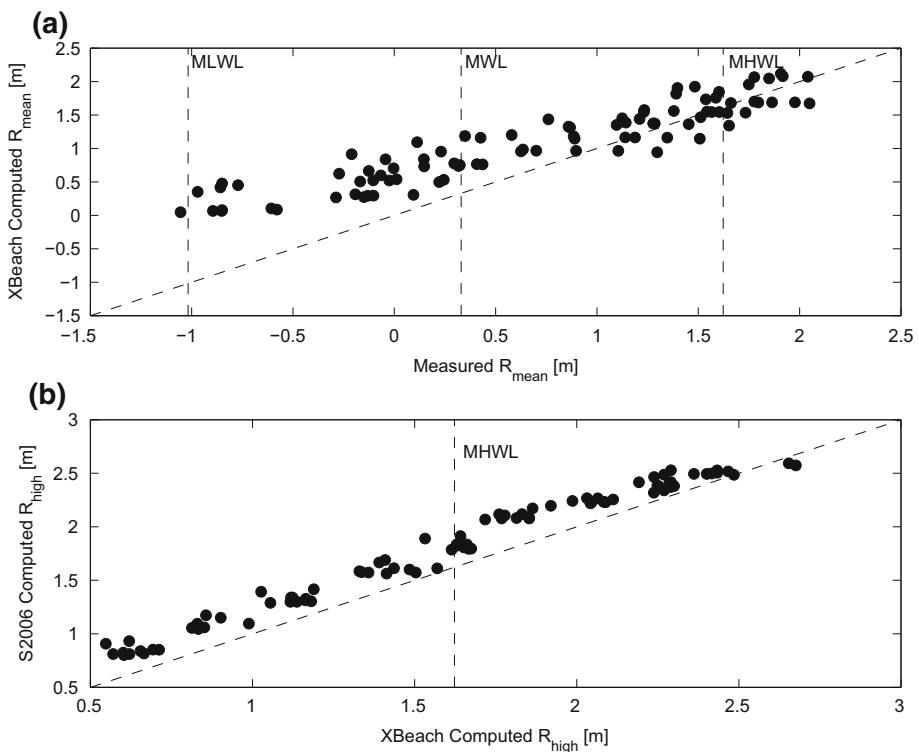

Fig. 6 **a** Comparison of observed and XBeach computed R_{mean}. **b** Comparison of XBeach computed and S2006 computed R_{high}. *Vertical black lines* correspond to the mean low water level (MLWL), mean water level (MWL) and mean high water level (MHWL)

at high tide (RMSE = 0.31 m). The main discrepancies appear at low tide where the computed R_{mean} is systematically higher than video derived R_{mean} (RMSE = 0.80m). It is hypothesized that for low tidal levels, the swash zone is very dissipative and its boundary is more diffuse than for higher tidal levels.

Therefore, the location of the colour intensity contrast between dry and wet pixels, which serves as a proxy to delineate the shoreline position, tends to be further offshore than the real mean water level. For higher water levels the swash zone is narrow, hence the contrast is much more pronounced and less widespread. The values of extreme water level R_{high} computed with Eq. 2 using both XBeach and S2006 are displayed in Fig. 6b. Overall, S2006 overestimates R_{high} compared with XBeach. The mean magnitude of R_{high} computed with S2006 is ~ 19 cm greater. The discrepancies between the two methods are smaller for the highest water levels.

4.4 SIR inferred from video images

The SIR were also estimated from the timex images recorded during the study period. The criterion of identification of a SIR was based on a visual analysis. The estimated SIR is assumed to be representative of the impact regime over this period. If the waterline, visually detectable, was below either the base of the seawall or the toe of the dune, it was assumed that the SIR corresponds to a swash regime (Fig. 7a, b). If the waterline was beyond these limits, collision regime was assigned (Fig. 7c, d). If the presence of water was detectable on the pathway of the engineered section of the beach, the SIR was set to overwash (Fig. 7e, f). All images were double checked by two different researchers to minimize the uncertainties in the detection method. Furthermore, at cases where the estimation of the SIR by means of timex images were not clear, also snapshot images were used as additional information. Unfortunately, the analysis was restricted to 86 images on a total of 268 available images. The limited number of usable images is linked to either low light, preventing us from clearly detecting the waterline limit, or malfunction of the video system, which could not operate during few days.

5 Results

5.1 Storm conditions

The nearshore wave characteristics during the study period (Fig. 8), which spans from the 1st to the 15th of February 2013 were calculated with the wave propagation model described in Sect. 3.1. Mean significant wave height, mean peak wave period and mean peak direction were $\overline{H_s} = 2.6$ m, $\overline{T_p} = 12.7$ s and $\overline{\theta_p} = 350°$, respectively. The alongshore variability was low, presenting mean standard deviations ($\overline{\sigma}$) of 0.12 m for H_s and 0.44 s for T_p. Following the definition of storm given in Sect. 3.2, the beach of Zarautz experienced three storm events of variable intensity and duration with one particularity severe storm (storm 2) with a maximum significant wave height (H_{max}) exceeding 6 m. The storm waves had a quasi shore-normal incidence. The return period of the H_s values recorded during the storm sequence was small (maximum return period of ~ 1 year).

Individual storm characteristics are summarized in Table 1. The duration of the storms was variable between 3.5 days for the longest (storm 2) and 1.45 days for the shortest (storm 1). The storms coincided with different tidal ranges with a maximum water level
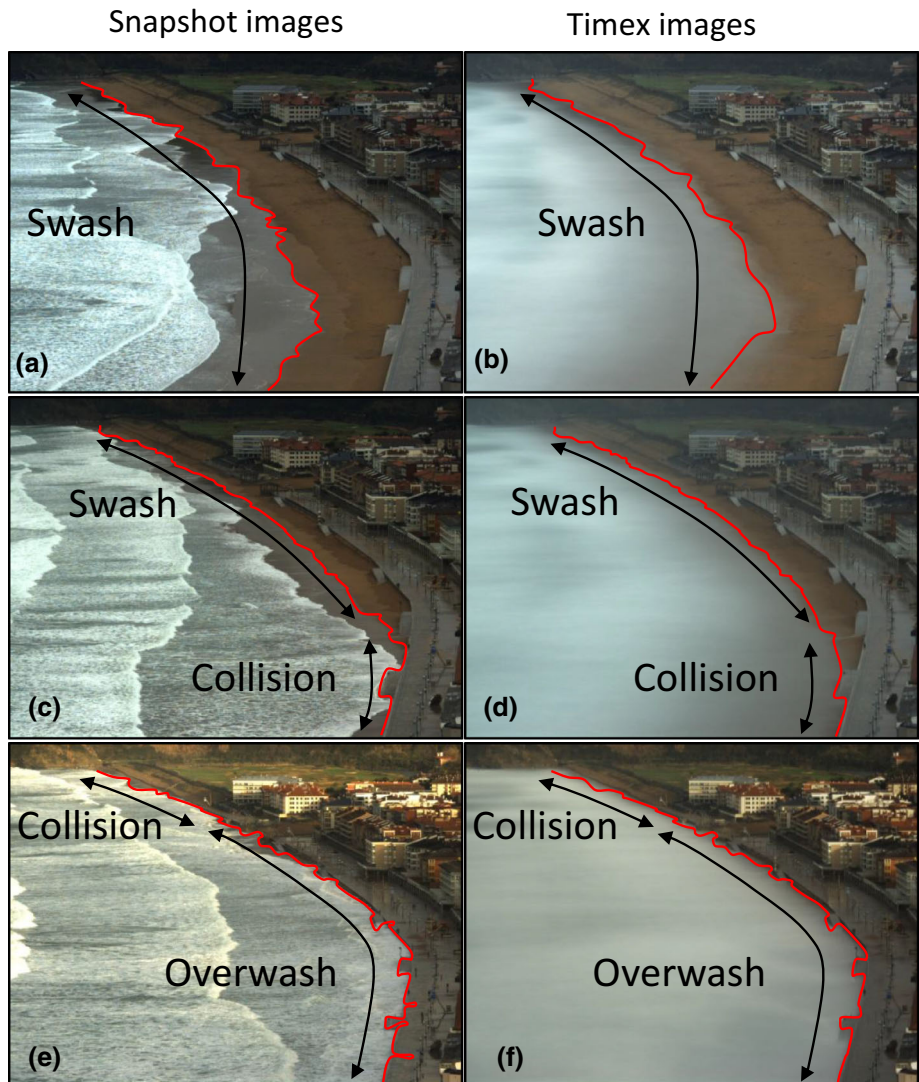
Snapshot images | Timex images

Fig. 7 Storm impact regime (SIR) estimated from the video monitoring system images. *Left panel* shows the SIR estimated by the snapshot images. *Right panel* shows the SIR estimated by the timex images. All images were captured during 11 February 2013

varying from 1 to 2.47 m at high tide. Storm 2 was the most powerful, presenting a maximum significant wave height of 6.3 m that coincided with a peak period of 17.2 s. The maximum significant wave height during storm 3 was similar to that of storm 2 ($H_{max} = 5.9$ m), but it had a shorter peak period ($T_p = 12.9$ s). This storm coincided with the largest tidal range of the storm sequence.
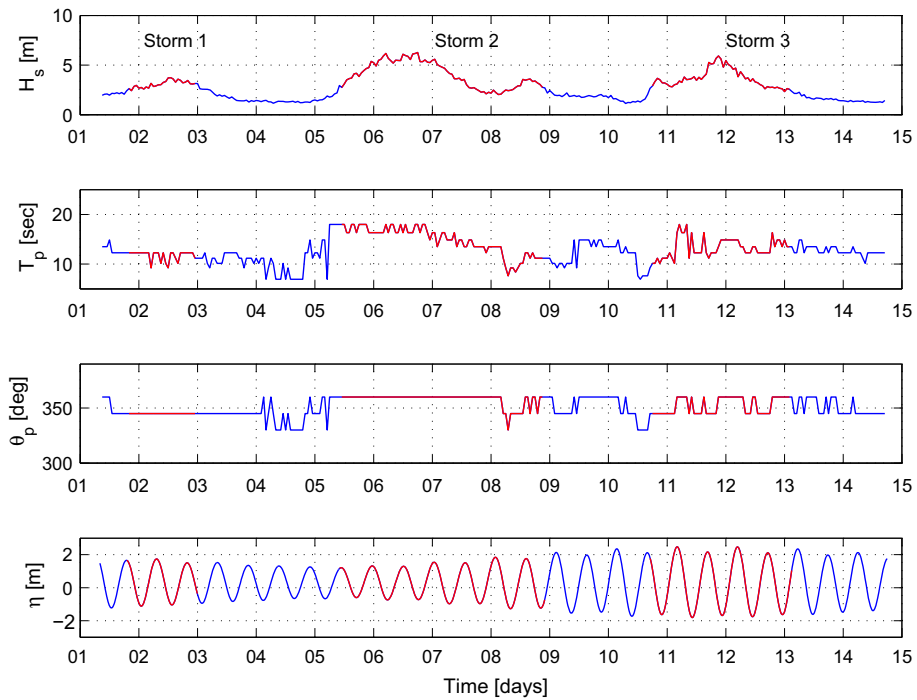
Fig. 8 Time series of nearshore wave conditions during the surveyed period. Storm events are highlighted by *red lines*

Table 1 Storm characteristics during the study period

Storm	H_{max} (m)	$\overline{T_p}$ (s)	Duration (h)	Storm P (Mw h/m)	η_{max} (m)
Storm 1	3.7	11.6	35	2	1.74
Storm 2	6.3	14.4	85	10.7	1.84
Storm 3	5.9	13	59	5.5	2.47

5.2 Comparison between observed and computed SIR

The SIR estimated from the video images are displayed in Fig. 9b together with the wave conditions and the water level (Fig. 9a). The blanks in Fig. 9b correspond to gaps in the video data set, related either to low light conditions (night) or camera malfunctions (between day 5 and 11). Therefore, images only cover partially storm 1 and storm 3. According to images, swash regime was dominant during the first 5 days at all profiles even under the storm conditions that prevailed during day 2. Collision regimes were detected during the storm 3 at high tide for day 11 and 12. From day 13 until day 15, collision was only detected at the western part of the beach at profiles 1–3 for wave conditions lower than the threshold values for storm conditions but during high tide. The detection of overwash regime occurrence was scarce and limited to the engineered section of the beach during storm 3.
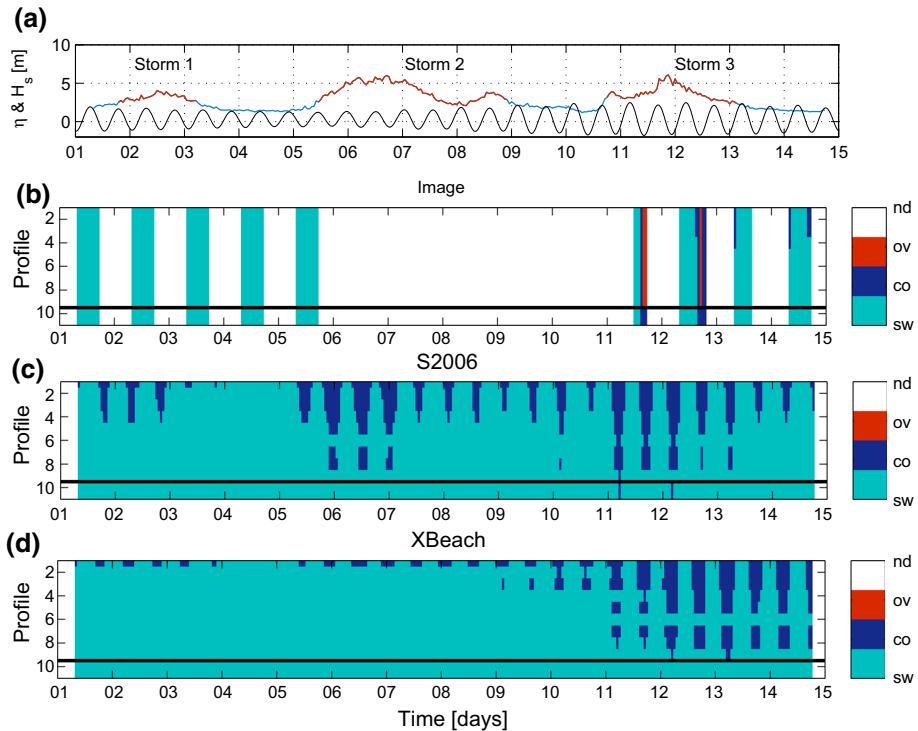
Fig. 9 Sallenger regime inferred from different approaches. **a** Wave and total water level data. Storm period highlighted by *red solid line*. **b** Sallenger regime inferred from camera images. **c** Sallenger regime inferred from S2006. **d** Sallenger regime inferred from XBeach. *Light blue colour* represents swash regime (sw). *Dark blue colour* represents collision regime (co). *Red colour* represents overwash regime (ov). *White colour* represents data gaps (nd). The *black horizontal line* delineates the limit between the engineered part and the natural part of the beach

SIR computed with Sallenger (Fig. 9c) and XBeach (Fig. 9d) show a strong modulation by the tide, especially for the occurrences of collision regime. Indeed, the majority of the computed collision regimes occur at high tide whatever the wave conditions and the method used. For profile 1, the two methods give similar results. Results differ for profiles 2–9 during the two first storms. SIR computed with S2006 alternate between swash and collision regimes, while SIR computed with XBeach are exclusively swash. From day 9 until the end of the study period, both methods give substantially similar results. Tidal modulation of the collision regime occurrence is clear. Collision regime computed with XBeach is present for nearly all the profiles of the engineered beach, except profile 6 where only swash is computed. SIR regimes computed with S2006 for profile 1–8 alternate between swash and collision until the end of storm 3, then collision regime only occur at profiles 1–3. Collision regime in the natural zone (profiles 10–11) is only computed with S2006 and coincide either with spring tide or the peak of the storm. No overwash regime was modelled neither with S2006 nor XBeach.

The skill of XBeach and S2006 to predict a correct SIR was computed using three indexes Hit, False and Miss (Fig. 10). These indexes are usually used in fluvial flooding studies (Alfieri et al. 2014; Bates and De Roo 2000) and more recently to assess model skill for coastal flooding applications (Vousdoukas (2016). The Hit ratio is a proxy of
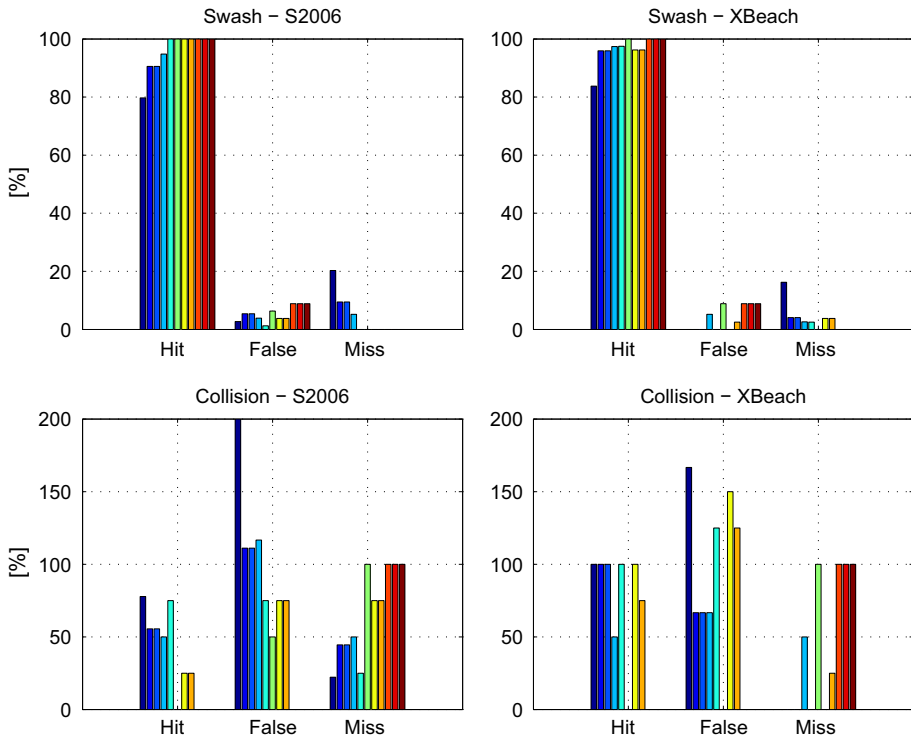
Fig. 10 Accuracy reproducing Sallenger regimes inferred from S2006 and XBeach based on Hit, False and Miss rates. Each *colour bar* correspond to a different beach profile. *Bluish* to *reddish colour bar* indicates profile locations from westward to eastward

model success reproducing a given SIR. It is defined as the number of times that model and observations agree, divided by the number of times a given SIR occurred. The False ratio is a proxy of model false alarms. It is computed dividing the number of times that model falsely predicts a given SIR by the times this really occurs. Finally, the model failure can be determined by the Miss index which a ratio between the number of times that model does not predict a given SIR and the times this really occurs. For swash regime, the SIR computed with S2006 and XBeach are in good agreement with SIR estimated from video images, nearly reaching the 100% of Hit ratio at each profile location. This agreement increases eastward for both methods. In the engineered section, the accuracy of XBeach is higher than S2006 (False = 0 for half of the profiles). Swash regime was not predicted by the two methods in very few cases and mainly at the western side of the engineered zone (Miss ≈ 20% for S2006 and Miss ≈ 16% for XBeach at profile 1). The Hit ratio for the collision regime are still high at the engineered section of the beach with a better accuracy for XBeach. However, the two methods overestimate the occurrence of collision regime and more particularly XBeach, as shown in Fig. 9. At the dune section (profile 10–11), collision regime was not predicted by XBeach (Miss = 100%). S2006 predicts collision regime during storm 3 (Fig. 9), but predicted events are not coinciding with observations explaining a 100% Miss ratio.

6 Discussion

Both methods give substantially similar results for the occurrence of swash regime and they mainly differ for the forecast of collision regime. If we only consider the period when images are available, S2006 tends to underestimate the occurrence of collision regime. However, if we now consider the whole study period, collision regimes computed with S2006 are more frequent than those computed with XBeach. In order to get a better insight of differences between the two methods, the evolution of the computed R_{high} values, used as a proxy in the Sallenger scale (Eq. 2), were compared for the entire study period in the following section.

6.1 Comparison of R_{high} computations

Figure 11 shows the evolution of R_{high} calculated from S2006 and XBeach for three different profiles P3, P8 and P10 (see Fig. 3 for profile location) representative of the alongshore variability of the shoreline. The profiles P3 and P8 are backed by the seawall. The initial dry beach width at profile P3 (~ 10 m) is much shorter than at profile P8 (~ 20 m). The profile P10 is backed by the sand dune.
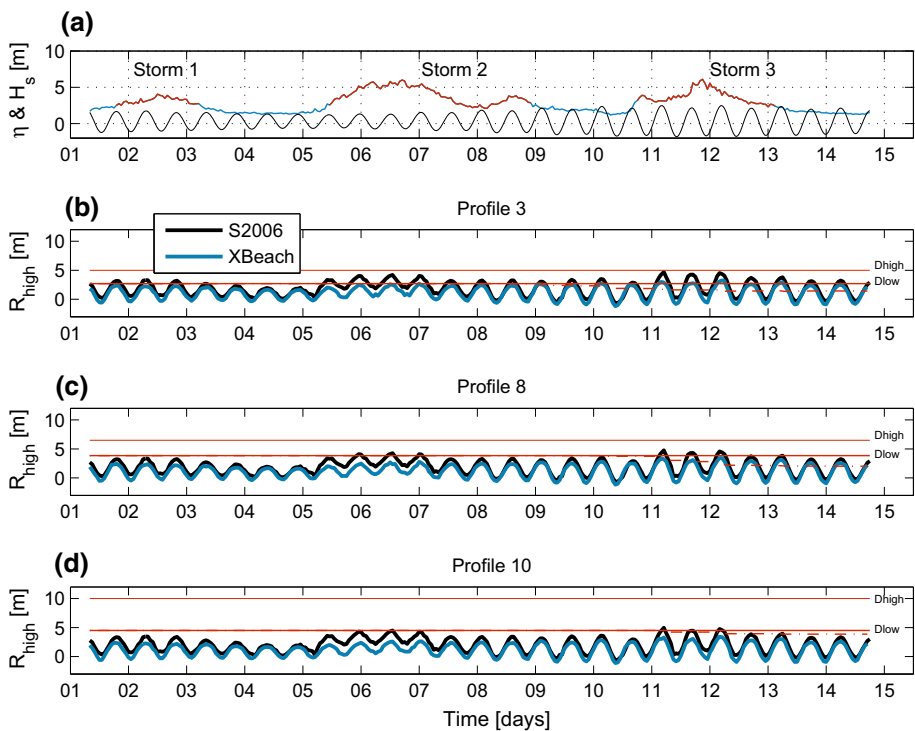

Fig. 11 Total water level (R_{high}) estimated by S2006 and XBeach approaches at profile 3, 8 and 10. **a** Wave and measured total water level data. **b–d** Total water level (R_{high}) calculated from S2006 and XBeach. The *horizontal red solid* D_{low} is used for the S2006 approach, while the *dashed one* is used for XBeach approach

Overall, the R_{high} values estimated with S2006 are larger than those calculated with XBeach whatever the profile location on the beach. The bias between the R_{high} obtained with S2006 and XBeach are ~ 0.7 m for P3–P8 and ~ 0.8 m for P10. This suggests that S2006 gives higher values of $R_{2\%}$ compared with XBeach predictions. Differences between those two methods were also documented in Stockdon et al. (2014). It was shown that discrepancies can increase when using a two-dimensional spatial domain in the XBeach model set-up as it was done in the present study. From a risk assessment point of view, the use of S2006 is more conservative at the engineered section of the beach at least for the two first storms.

The differences between R_{high} computed with S2006 and XBeach are similar at profile 3 and 8. The greater differences are found during storms 2 and 3. During storm 1, both methods give very close values of R_{high} . However, since S2006 overestimates $R_{2\%}$ it is more prone to give R_{high} values greater or equal to D_{low} leading to a dominant collision SIR. At profile 8, since the beach width is two times greater than at profile 3, the difference of R_{high} computed with S2006 and XBeach has less influence on the SIR forecast for storm 1. For the more energetic wave conditions during storms 2 and 3 differences are larger leading to different SIR if we consider a fixed D_{low}. However, it is worthy to note a lowering of the elevation of D_{low} computed with XBeach (red dashed line in Fig. 11). While in S2006 the beach slope is fixed during the all computation, XBeach allows to simulate the bed changes and the coupling with the hydrodynamics processes. In S2006, runup is computed assuming an infinite sloping beach. This formulation is appropriate as far as R_{high} is lower than D_{low}. Once the runup reaches the base of the seawall it is not possible to precisely discriminate between a collision and an overwash SIR. For the study, SIR was always set to collision regime when R_{high} obtained from S2006 was higher than D_{low} and smaller or equal than D_{high}. This means that in this case, the risk of overwash of the pathway might have been underestimated. XBeach is supposed to overcome this limitation. However, wave conditions during the study period were not energetic enough to observe flooding of the pathway. Only few events of wave overtopping were eye witnessed.

At profile P10, R_{high} values computed with XBeach are always lower than values obtained with S2006 (Fig. 11) and lower than D_{low}. As a result, the SIR estimated by XBeach was set to swash regime during the entire study period (Fig. 9) at this location. This assessment would mean that the dune was not eroded. However, the topographic measurements carried out during the study period indicate that the dunes suffered erosion. Indeed, the volume of eroded dune was estimated at 10.13 m^3/m. In addition, the occurrence of collision regimes was estimated from video images (Fig. 9) at high tide during days 11 and 12, likely producing the dune erosion. Collision regime was also assessed using S2006 to compute R_{high} during the same days but at different times also coinciding with high tide. This result suggests that limiting the use of R_{high} as a proxy to assess SIR using XBeach can lead to a misestimation of the risk of dune erosion. Indeed, the analysis of the bed changes computed with XBeach show that the dune erosion was predicted by the model. The eroded volume was estimated at 2.44 m^3/m. This suggests that even if XBeach gives lower values of $R_{2\%}$ than S2006, it is able to capture the main processes that control the dune erosion. Dune erosion is usually the result of successive swash events that weaken the dune toe by removing sand and steepening the dune slope until reaching a critical angle that leads to dune avalanching. This process is included in XBeach through an avalanching algorithm (Roelvink et al. 2009).

6.2 Simulation of different storms scenario

Four different storms scenario were designed in order to test the two methods for wave and tidal conditions different than those of the study period (Table 2). All simulations lasted 48 h, which corresponds to the mean duration of storms at the study site. Two different wave scenarios were considered. The first scenario (case 1 and case 2) corresponds to 1-year

Table 2 Wave and tide characteristics of the test cases

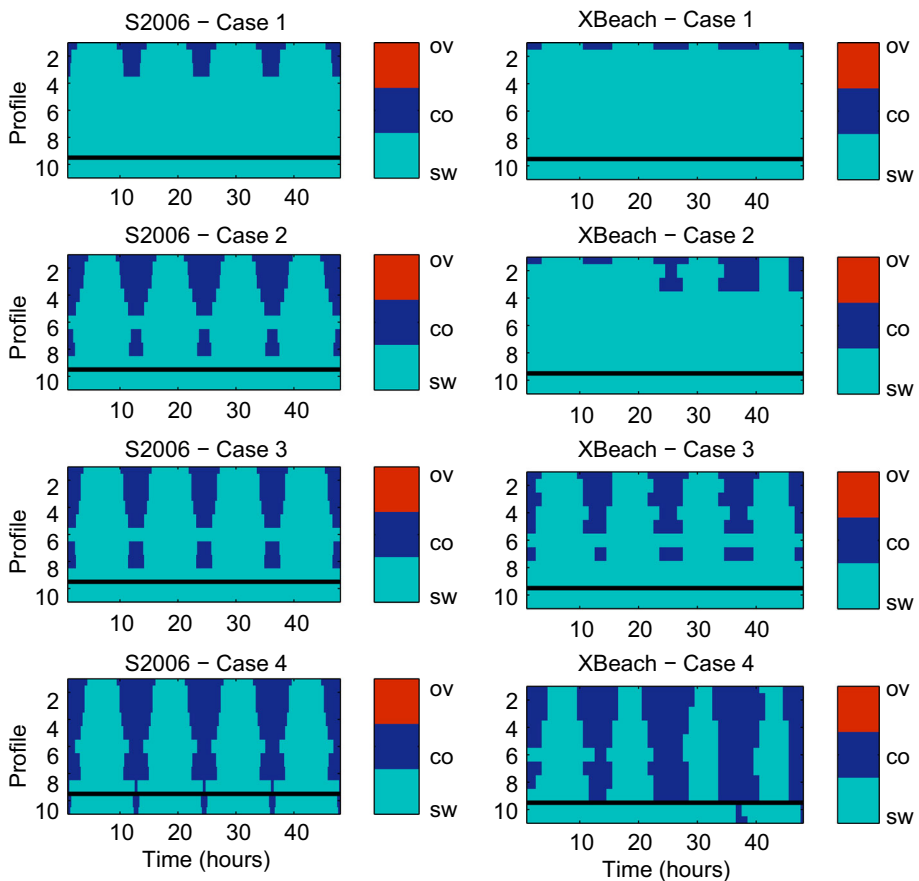|	H_s (m)	T_p (s)	Tide	Tidal range (m)
Case 1	5.65	12.5	Neap tide	1.9
Case 2	5.65	12.5	Spring tide	3.7
Case 3	7.86	14.5	Neap tide	1.9
Case 4	7.86	14.5	Spring tide	3.7

Fig. 12 Sallenger regime inferred from S2006 (*left panels*) and XBeach (*right panel*) for the four test cases. *Light blue colour* represents swash regime (sw). *Dark blue colour* represents collision regime (co). *Red colour* represents overwash regime (ov). The *black horizontal line* delineates the limit between the engineered part and the natural part of the beach

return period wave conditions, while the second and more energetic scenario is representative of wave conditions with a 10-year return period. The tidal conditions for cases 1 and 3 (cases 2 and 4) were set to neap tide (spring tide). The wave conditions were maintained constant during the whole simulation. The XBeach parameters used for the present simulations were the same as the obtained in the calibration of the model (see Sect. 4.3.1 for more information).

At the engineered section of the beach, the variability of SIR calculated with both methods shows a strong modulation by the tide for all the cases (Fig. 12). SIR alternate between swash regime at low water levels and collision regime during high water levels. Furthermore, wave conditions seem to control the alongshore variability of SIR. Indeed, for the same tidal range (case 1 vs. case 3 and case 2 vs. case 4), the number of profiles where collision regimes are computed increase with the storm intensity. This result can be explained by the shape of the beach. The beach width shrinks at the western side (Fig. 3) which leads to a reduction in the extension of the swash zone. Therefore, computed R_{high} is more prone to exceed D_{low} than on the rest of the beach.

For case 1 and case 2, collision regimes would occur at almost all the profiles using S2006, while XBeach would tend to limit the occurrence of collision regimes to profile 1–3. It is worthy to mention that the occurrence of collision regimes at a given location increases after 24 h with XBeach while the collision regime pattern computed with S2006 is similar during the whole simulation. This result highlights the influence of the bed
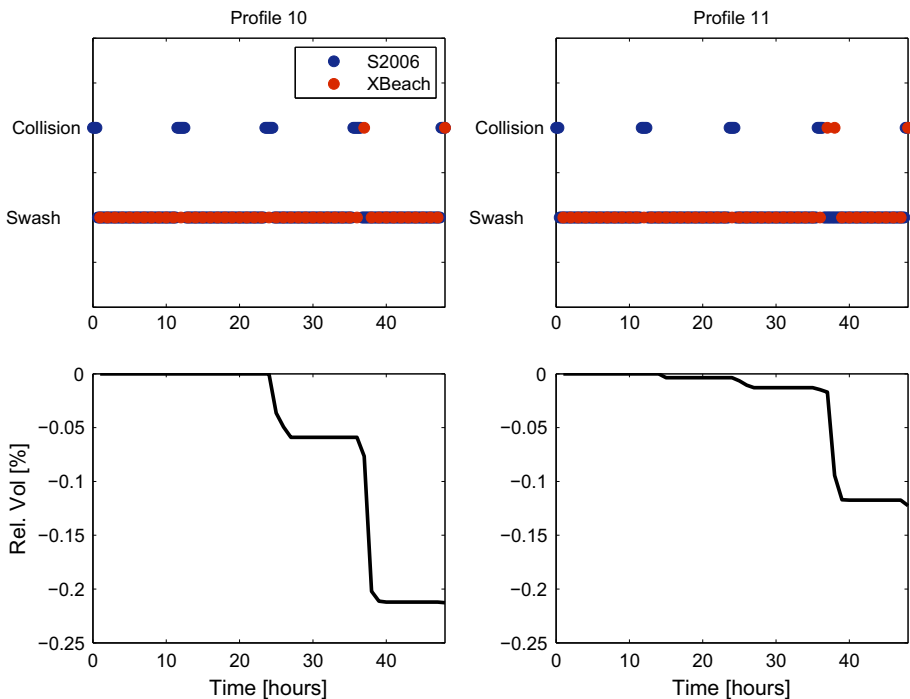

Fig. 13 (*Top*) Sallenger regime inferred from S2006 (*blue dots*) and XBeach (*red dots*) for test case 4. (*Bottom*) Dune volume evolution modelled by the XBeach model. The dune volume evolution is represented as relative dune volume $\left(100 \times \frac{\mathrm{Vol}_{t_n} - \mathrm{Vol}_{t_1}}{\mathrm{Vol}_{t_1}} \right)$

changes during storms which could influence the magnitude of the runup and thus the intensity of storm impacts.

For cases 1, 2 and 3, the section of the beach backed by the dune would only experience swash regime. Collision regimes, which would mean a potential risk of erosion of the dune, would only occur during the case 4 scenario. It would occur for all high tides according to S2006, but only at the last tidal cycle according to XBeach results. The analysis of the relative dune volume $\left(100 \times \frac{\text{Vol}_{t_n} - \text{Vol}_{t_1}}{\text{Vol}_{t_1}}\right)$ changes computed with XBeach (Fig. 13) shows that the dune would have suffered from erosive events sooner. However, their occurrence would have been less frequent than predicted by S2006.

7 Conclusion

The main purpose of the present paper was to test two methods to estimate SIR based on the Sallenger scale to provide some guidelines to coastal managers. These two methods were applied in a partially engineered beach, which can be considered representative of most of the urbanized beaches. A wide range of tools and data (orthorectified video images, topographic surveys and numerical simulations) were combined to provide nearshore wave conditions and an estimation of impact regimes during a series of 3 storms that battered the study site during 2 weeks. The principal results are resumed in the following:

- The parametric method that uses the S2006 formulation to compute $R_{2\%}$ is relatively simple, requires a low computational cost (instantaneous results) and only few input parameters are needed to run the model.
- This type of model does not solve all the physical processes involved during the storm (wave propagation, wave generated currents, sediment stirring etc.). By consequence, the bed changes that occur in the course of a series of closely spaced storms are not accounted for in the computation of the evolution of $R_{2\%}$.
- The S2006 formulation needs to be modified to integrate the effect of seawalls especially to be able to predict pathway overwash at engineered beaches.
- The XBeach process-based model is complex, requires a relatively high computational cost and the number of input parameters needed to run the model is large and sometimes hard to obtain (e.g. pre-storm bathymetry). Furthermore, it is site specific as it needs a proper calibration in order to obtain realistic results.
- This kind of model solves all the physical processes involved during the storm. This allows to compute not only $R_{2\%}$ but also the beach evolution during the course of a storm. Thus, this model is more than enough to perform simple risk analysis.
- The comparisons between the two methods show that if they were integrated in an operational EWS, the system based on S2006 will be more conservative than using XBeach, at least at the section of the beach backed by the dune. However, the combination of the two methods can provide a more flexible and accurate EWS that can use the conservative model as a fast indicator to run the more complex model.
- Finally, the XBeach model appears to be more appropriated for anticipating extreme storm scenario allowing to test the efficiency of risk mitigation and management procedures to assist coastal authorities.

References

Aarninkhof S, Turner I, Dronkers T, Caljouw M, Nipius L (2003) A video-based technique for mapping intertidal beach bathymetry. Coast Eng 49(4):275–289

Aarninkhof S, Ruessink B, Roelvink J (2005) Nearshore subtidal bathymetry from time-exposure video images. J Geophys Res Oceans (1978–2012) 110(C6):C06011

Alfieri L, Salamon P, Bianchi A, Neal J, Bates P, Feyen L (2014) Advances in pan-European flood hazard mapping. Hydrol Process 28(13):4067–4077

Almeida L, Vousdoukas M, Ferreira Rodrigues B, Matias A (2012) Thresholds for storm impacts on an exposed sandy coastal area in Southern Portugal. Geomorphology 143144:3–12

Austin MJ, Scott TM, Russell PE, Masselink G (2012) Rip current prediction: development, validation, and evaluation of an operational tool. J Coast Res 29(2):283–300

Bates PD, De Roo A (2000) A simple raster-based model for flood inundation simulation. J Hydrol 236(1):54–77

Beevers L, Popescu I, Pan Q, Pender D (2016) Applicability of a coastal morphodynamic model for fluvial environments. Environ Model Softw 80:83–99

Bengtsson L, Hodges KI, Keenlyside N (2009) Will extratropical storms intensify in a warmer climate? J Clim 22(9):2276–2301

Castelle B, Marieu V, Bujan S, Splinter KD, Robinet A, Senechal N, Ferreira S (2015) Impact of the winter 2013–2014 series of severe Western Europe storms on a double-barred sandy coast: beach and dune erosion and megacusp embayments. Geomorphology 238:135–148

Ciavola P, Ferreira O, Haerens P, Van Koningsveld M, Armaroli C (2011a) Storm impacts along European coastlines. Part 2: Lessons learned from the MICORE project. Environ Sci Policy 14(7):924–933

Ciavola P, Ferreira O, Haerens P, Van Koningsveld M, Armaroli C, Lequeux Q (2011b) Storm impacts along European coastlines. Part 1: The joint effort of the MICORE and CONHAZ projects. Environ Sci Policy 14(7):912–923

Coco G, Senechal N, Rejas A, Bryan KR, Capo S, Parisot J, Brown J, MacMahan J (2014) Beach response to a sequence of extreme storms. Geomorphology 204:493–501

Cohn N, Ruggiero P (2016) The influence of seasonal to interannual nearshore profile variability on extreme water levels: modeling wave runup on dissipative beaches. Coast Eng 115:79–92

de Santiago I (2014) Storm impact on engineered pocket beaches. PhD thesis, Université de Pau et des Pays de l'Adour

de Santiago I, Morichon D, Abadie S, Liria P, Epelde I (2013) Video monitoring nearshore sandbar morphodynamics on a partially engineered embayed beach. J Coast Res 65:458–463

Dolan R, Davis RE (1992) An intensity scale for Atlantic coast northeast storms. J Coast Res 8(4):840–853

Dorsch W, Newland T, Tassone D, Tymons S, Walker D (2008) A statistical approach to modelling the temporal patterns of ocean storms. J Coast Res 24(6):1430–1438

Ferreira Ó (2005) Storm groups versus extreme single storms: predicted erosion and management consequences. J Coast Res 42:221–227

Guimarães PV, Farina L, Toldo E, Diaz-Hernandez G, Akhmatskaya E (2015) Numerical simulation of extreme wave runup during storm events in Tramandaí Beach, Rio Grande do Sul, Brazil. Coast Eng 95:171–180

Holland K, Raubenheimer B, Guza R, Holman RA (1995) Runup kinematics on a natural beach. J Geophys Res Oceans 100(C3):4985–4993

Holman R (1986) Extreme value statistics for wave run-up on a natural beach. Coast Eng 9(6):527–544

Holman R, Guza R (1984) Measuring run-up on a natural beach. Coast Eng 8(2):129–140

Karunarathna H, Pender D, Ranasinghe R, Short AD, Reeve DE (2014) The effects of storm clustering on beach profile variability. Mar Geol 348:103–112

Kirby JT, Dalrymple RA, Kaku H (1994) Parabolic approximations for water waves in conformal coordinate systems. Coast Eng 23(3):185–213

Longuet-Higgins MS, Stewart R (1963) A note on wave set-up. J Mar Res 21:4–10

Loureiro C, Ferreira Ó, Cooper JAG (2012) Extreme erosion on high-energy embayed beaches: influence of megarips and storm grouping. Geomorphology 139:155–171

Morris J (2013) Estimation of the nearshore bathymetry using remote sensing techniques. Master's thesis, Delft University of Technology, Delft

Morton RA (2002) Factors controlling storm impacts on coastal barriers and beaches: a preliminary basis for near real-time forecasting. J Coast Res 18(3):486–501

Nielsen P, Hanslow DJ (1991) Wave runup distributions on natural beaches. J Coast Res 7(4):1139–1152

Oke TR (1987) Boundary layer climates, vol 5. Psychology Press, Stockholm

O'Reilly W, Guza RT (1993) A comparison of two spectral wave models in the Southern California bight. Coast Eng 19(3):263–282

Poelhekke L, Jäger WS, van Dongeren A, Plomaritis TA, McCall R, Ferreira Ó (2016) Predicting coastal hazards for sandy coasts with a Bayesian network. Coast Eng 118:21–34

Poelhekke L, Jäger WS, van Dongeren A, Plomaritis TA, McCall R, Ferreira Ó (2016) Predicting coastal hazards for sandy coasts with a Bayesian network. Coast Eng 118:21–34

Rangel-Buitrago N, Anfuso G (2011b) Morphological changes at Levante Beach (Cádiz, SW Spain) associated with storm events during the 2009–2010 winter season. J Coast Res 64:1886–1890

Raubenheimer B, Guza R (1996) Observations and predictions of run-up. J Geophys Res Oceans (1978–2012) 101(C11):25575–25587

Roelvink D, Reniers A, van Dongeren A, van Thiel de Vries J, McCall R, Lescinski J, (2009) Modelling storm impacts on beaches, dunes and barrier islands. Coast Eng 56(11):1133–1152

Ruessink B, Kleinhans M, den Beukel P (1998) Observations of swash under highly dissipative conditions. J Geophys Res Oceans (1978–2012) 103(C2):3111–3118

Sallenger AH Jr (2000) Storm impact scale for barrier islands. J Coast Res 6(3):890–895

Sasso R (2012) Video-based nearshore bathymetry estimation for rip current forecasting on a macro-tidal beach. Master's thesis, Delft University of Technology, Delft

Senechal N, Coco G, Bryan KR, Holman RA (2011) Wave runup during extreme storm conditions. J Geophys Res Oceans 116(C7):C07032

Smit M (2010) Formation and evolution of nearshore sandbar patterns. PhD thesis, Delft University of Technology Delft

Splinter KD, Carley JT, Golshani A, Tomlinson R (2014) A relationship to describe the cumulative impact of storm clusters on beach erosion. Coast Eng 83:49–55

Stockdon HF, Holman RA, Howd PA, Sallenger AH Jr (2006) Empirical parameterization of setup, swash, and runup. Coast Eng 53(7):573–588

Stockdon HF, Thompson DM, Plant NG, Long JW (2014) Evaluation of wave runup predictions from numerical and parametric models. Coast Eng 92:1–11

Van Dongeren A, Svendsen IA (1997) Absorbing-generating boundary condition for shallow water models. J Waterw Port Coast Ocean Eng 123(6):303–313

Van Dongeren A, Plant N, Cohen A, Roelvink D, Haller MC, Catalán P (2008) Beach wizard: nearshore bathymetry estimation through assimilation of model computations and remote observations. Coast Eng 55(12):1016–1027

van Koningsveld M, Davidson MA, Huntley DA (2005) Matching science with coastal management needs: the search for appropriate coastal state indicators. J Coast Res 21(3):399–411

Van Thiel de Vries JSM, Van Gent MRA, Walstra DJR, Reniers AJHM (2008) Analysis of dune erosion processes in large-scale flume experiments. Coast Eng 55(12):1028–1040

Vitorino J, Oliveira A, Jouanneau J, Drago T (2002) Winter dynamics on the northern portuguese shelf. Part 1: Physical processes. Prog Oceanogr 52:129–153

Vousdoukas MI (2014) Observations of wave run-up and groundwater seepage line motions on a reflective-to-intermediate, meso-tidal beach. Mar Geol 350:52–70

Vousdoukas MI (2016) Developments in large-scale coastal flood hazard mapping. Nat Hazards Earth Syst Sci 16(8):1841

Vousdoukas MI, Almeida LPM, Ferreira Ó (2012a) Beach erosion and recovery during consecutive storms at a steep-sloping, meso-tidal beach. Earth Surf Proc Land 37(6):583–593

Vousdoukas MI, Ferreira Ó, Almeida LP, Pacheco A (2012b) Toward reliable storm-hazard forecasts: XBeach calibration and its potential application in an operational early-warning system. Ocean Dyn 62(7):1001–1015

Williams JJ, de Alegría-Arzaburu AR, McCall RT, Van Dongeren A (2012) Modelling gravel barrier profile response to combined waves and tides using XBeach: laboratory and field results. Coast Eng 63:62–80

Woolf DK, Challenor P, Cotton P (2002) Variability and predictability of the North Atlantic wave climate. J Geophys Res Oceans 107(C10):9-1–9-14

Wooster W, Bakun A, McLain D (1976) The seasonal upwelling cycle along the eastern boundary of the North Atlantic. J Mar Res 34(2):131–141

Wright L, Short AD (1984) Morphodynamic variability of surf zones and beaches: a synthesis. Mar Geol 56(1–4):93–118